Study of Power End Peaking for NRU Loop Fuel Calculations

T.S. Nguyen and R.E. Donders
AECL Chalk River Laboratories, Chalk River, Ontario, Canada

Abstract

End-flux peaking effects in fuel bundles irradiated in the NRU (National Research Universal reactor) loop test sections are investigated using MCNP (the Monte Carlo N-Particle transport code). The current method for calculating powers in the loop bundles only allows for an integrated end-power-peaking correction. In this paper, an element axial power ratio (APR), determined as the 3D MCNP-calculated fission power at an element axial location relative to the 2D WIMS (Winfrith Improved Multigroup Scheme lattice transport code) power, is introduced. This may be used, as supplementary information to BURFEL (the Burnup of Fuel Elements code and database system), to obtain the accurate axial distributions of element powers, thereby, enabling the quantification of those element-end power increases that are important for design of bundles and safety analysis.

1. Introduction

The flux of neutrons inducing fissions in a fuel element is known to increase at the fuel stack ends (referred to as *end-flux peaking*), or generally, wherever the fuel is axially adjacent to materials (either fuel or non-fuel) with a lower neutron absorption cross section. Where such end-flux peaking effects occur, the element fission power tends to increase (referred to as *end-power peaking*). Conversely, the fission power in fuel adjacent to a stronger neutron absorber may decrease instead.

Most computations of fuel powers in nuclear reactors are based on 2D neutronic models; so end-peaking powers are not calculated. However, in the majority of reactors, fuel elements extend through the whole core and end in such a low flux level that the end-element power increases are still small as compared to the mid-element powers. Even in CANDU®[1], where fuel channels contain a number of short fuel bundles and the end-peaking effects may occur in high flux regions, the end-peaking powers are insignificant due to the relatively small absorption cross section of the fuel, the small gaps between the fuel stacks of adjacent bundles, and the relatively low power ratings of natural uranium fuels [1]. The end-peaking effects are much greater if a CANDU-like channel contains fuel elements with high enrichment or strong poisons. That is the case with some loop irradiations in NRU (the National Research Universal reactor). Neglecting such end-peaking power increases in the subsequent thermalhydraulic analysis may result in significant underestimations of the fuel temperatures near element ends.

NRU is equipped with several vertical in-core sites, the loop test sections, cooled by pressurized light water, each of which can be loaded with six modified CANDU bundles axially held together in a so-called fuel string.

[1] CANDU® - a registered trademark of AECL.

As for loop fuel calculations at the Chalk River Laboratories, BURFEL (Burnup of Fuel Elements) has been used since the 1970s both to predict the element heating powers before insertion for irradiation and to obtain the powers and burnups in the fuel elements irradiated in NRU. As a method based on a 1D axial profile and a 2D radial calculation, BURFEL is not able to provide the detailed power profile at the end regions of the fuel.

End-peaking effects in loop fuels have been made (*e.g.*, [2]), especially for bundles containing enriched fuel elements and poisons. Some of these results have been used to derive the so-called element *end-power peaking ratios* (EPPR) as implemented in the current version of BURFEL. This does not, however, provide an accurate power profile or burnup near the fuel stack ends.

2. BURFEL

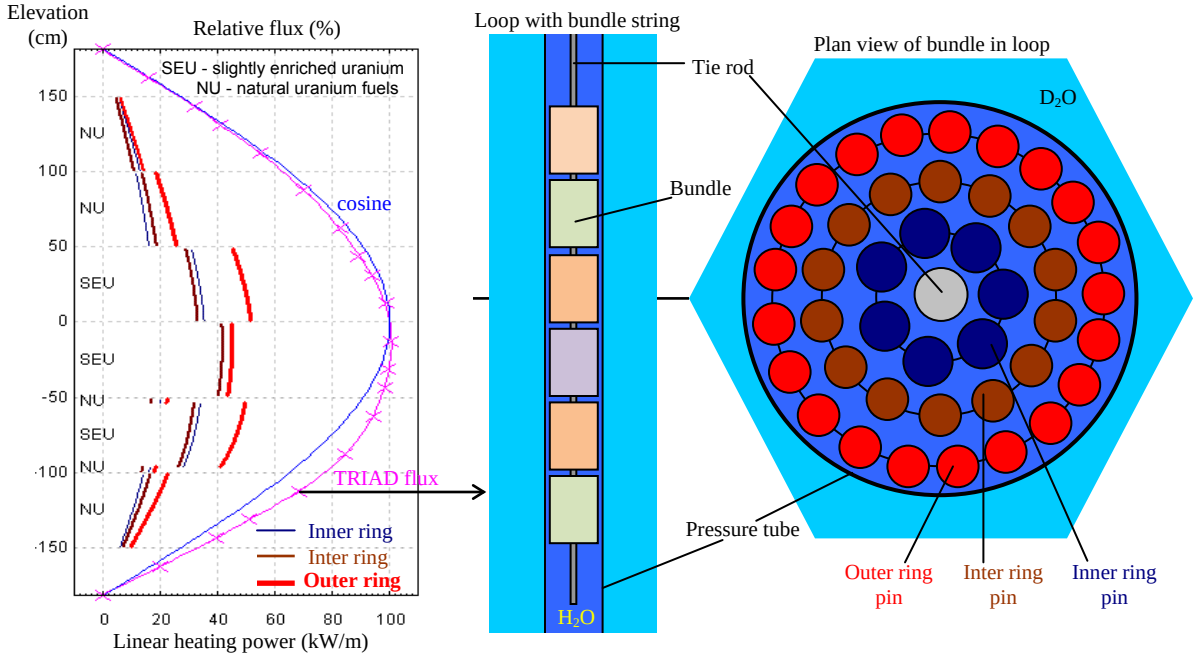

Figure 1 BURFEL model of NRU loop fuel string.

The BURFEL code calculates powers, burnups, fast-flux data, and coolant conditions for fuels irradiated in channels. The code is used for NRU loop irradiations, but could be used for CANDU channels. Figure 1 shows the basic geometry applicable to the BURFEL code, and gives an example of a power profile produced by BURFEL. The code can handle very general geometries. Each channel can contain an arbitrary number of bundles (the collection of bundles is called a fuel string), each bundle can be subdivided into an arbitrary number of "axial regions" (so that the parts of the bundle with end-pellets can be explicitly modeled), and each bundle region can be subdivided into an arbitrary number of axial "segments" (so that the axial profiles of the powers and burnups along the bundle regions can be calculated). The number of fuel elements within each region is arbitrary as well. This ability to handle complex geometries is needed since NRU loop irradiations often contain heterogeneous bundles with end-pellets.

Examples of BURFEL outputs are given in Tables 1 - 4.

Table 1 Summary of bundle and string powers for a typical NRU loop irradiation

Irradiation Full Power Days = 10.0.

Bundle	From Fission		Pin Heating		To Coolant	
	Energy (MWd)	Power (kW)	Energy (MWd)	Power (kW)	Energy (MWd)	Power (kW)
Z42A	2.05	205.1	1.95	195.2	1.98	198.2
Z36A	3.51	351.3	3.35	335.0	3.40	339.9
Z42B	8.86	885.5	8.28	828.4	8.39	838.9
Z30A	6.63	663.3	6.21	621.3	6.31	630.8
Z42C	7.80	779.8	7.30	730.4	7.40	739.7
Z36B	2.61	260.9	2.49	248.9	2.52	252.5
Total	31.46	3146.0	29.59	2959.2	30.00	3000.0

Table 2 Example of fuel power and burnup data produced by BURFEL

String Position # / Bundle Mid-Plane Elevation / Bundle ID / Orientation	Bundle Region	Inner Ring				Outer Ring			
		Pin ID / # of Pins / Fissile Enrichment	Segment Mid-Plane Elevation (cm)	Segment Linear Heating Power (kW/m)	Segment Burnup At EOI* (MWh/ kgIHE)	Pin ID / # of Pins / Fissile Enrichment	Segment Mid-Plane Elevation (cm)	Segment Linear Heating Power (kW/m)	Segment Burnup At EOI* (MWh/ kgIHE)
1, 125 cm, Z42A-Build1, Up	1	Inner, 7, 0.71%	141.0	7.1	1.5	Outer, 21, 0.71%	141.0	7.9	2.4
			125.0	9.6	2.0		125.0	10.6	3.2
			109.0	11.9	2.5		109.0	13.2	4.0
2, 75 cm, Z36A-Build1, Up	1	Inner, 6, 0.71%	91	12.6	2.9	Outer, 18, 0.71%	91	20.2	4.7
			75	14.2	3.2		75	22.7	5.3
			59	16.2	3.5		59	24.8	5.8
3, 25 cm, Z42B-Build1, Up	1	Inner, 7, 2.26%	41	32.1	7.0	Outer, 21, 2.26%	41	14.8	46.8
			25	35.1	7.4		25	15.5	49.3
			9	36.4	7.7		9	16.1	51.1
4, -25 cm Z30A-Build1, Up	1	NA	NA	NA	NA	Outer, 18, 1.25%	-9.4	45.1	10.8
							-25.0	45.0	10.7
							-40.6	44.3	10.6
5, -75 cm Z42C-Build1, Up	1	Inner, 7, 0.71%	-52.5	20.2	4.2	Outer, 21, 0.71%	-52.5	22.4	6.8
	2	Inner, 7, 2.26%	-61.0	33.4	7.3	Outer, 21, 2.26%	-61.0	48.8	15.4
			-75.0	31.9	7.0		-75.0	46.6	14.7
			-89.0	29.7	6.5		-89.0	43.3	13.7
	3	Inner, 7, 0.71%	-97.5	16.5	3.5	Outer, 21, 0.71%	-97.5	18.4	5.6
6, -125 cm, Z36B-Build1, Up	1	Inner, 6, 0.71%	-109	13.1	3.0	Outer, 18, 0.71%	-109	20.9	4.9
			-125	10.6	2.4		-125	16.9	4.0
			-141	7.8	1.8		-141	12.4	2.9

* EOI - end-of-irradiation period.

Table 3 Example of flux data produced by BURFEL

Elevation (cm)	Bundle ID / Region	>1 MeV Flux (1E17 n.m^{-2}.s^{-1})				>1 MeV Fluence (1E23 n.m^{-2}) Over Irradiation Period			
		Pressure Tube	Insert* 1		Insert 3	Pressure Tube	Insert 1		Insert 3
140	Z42A, 1	0.71				0.62			
132.5	Z42A, 1	0.83				0.72			
125	Z42A, 1	0.94				0.81			
117.5	Z42A, 1	1.1				0.91			
110	Z42A, 1	1.2				1.00			
Lines removed									
-10	Z30A, 1	3.1	4.1		4.5	2.6	3.5		3.9
-17.5	Z30A, 1	3.1	4.1		3.0	2.6	3.5		2.6
-25	Z30A, 1	3.0	4.1		3.5	2.6	3.5		3.0
-32.5	Z30A, 1	3.0	4.0		4.5	2.6	3.5		3.8
-40	Z30A, 1	3.0	4.0		4.4	2.6	3.5		3.8
-60	Z42C, 2	3.8				3.3			
-67.5	Z42C, 2	3.8				3.3			
Lines removed									

* Inserts are holders for material specimens irradiated in the “materials test bundles”.

Table 4 Example of coolant conditions produced by BURFEL

Bundle Position Number	Bundle Name	Hydraulic Position Number	Hydraulic Type	Heating *kW*	Elevation *cm*	Predicted		
						Temperature *°C*	Pressure *MPa*	Density *g/cm^3*
Outlet		8	U1B_Out	0.000	Bottom + ε	303.02	9.501	0.7075
1	Z42A	7	42EL	198.199	150.0 − ε	303.00	9.493	0.7075
					125.0	301.98	9.507	0.7100
					100.0 + ε	300.96	9.521	0.7123
Lines removed								
4	Z30A	4	MTB	630.783	0.0 − ε	288.32	9.613	0.7394
					-25.0	284.84	9.634	0.7464
					-50.0 + ε	281.36	9.654	0.7532
5	Z42C	3	42EL	739.699	-50.0 − ε	281.35	9.681	0.7532
					-75.0	277.15	9.694	0.7611
					-100.0 + ε	272.95	9.708	0.7687
Lines removed								
Inlet		1	U1B_In	0.000	Top − ε	270.01	9.770	0.7739

ε – an infinitesimal distance

Input and output data from BURFEL are maintained in relational databases. These databases facilitate the management of the BURFEL data. The structure of the output database is shown in Figure 2. Managing the data in databases greatly facilitates data extraction. For example, the

power histories of the fuels in a specific bundle, as shown in Table 5 and Figure 3, can be easily extracted using a simple database query.

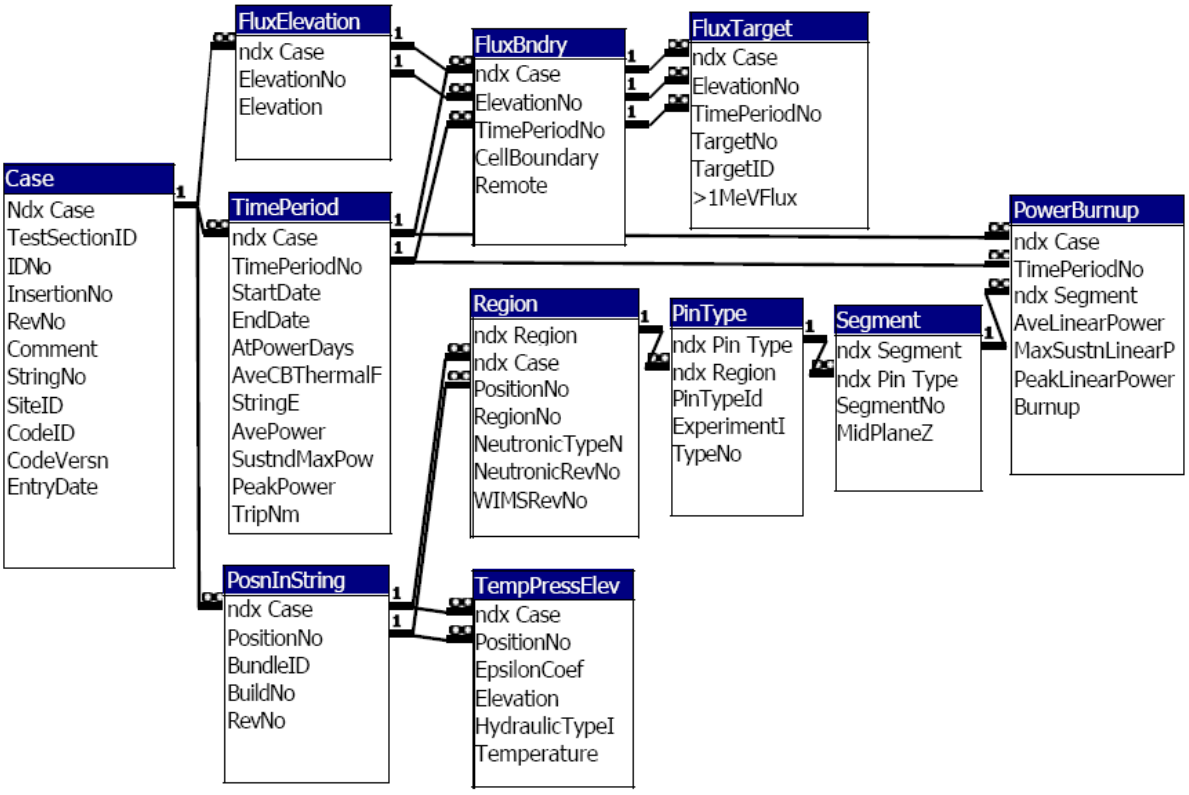

Figure 2 Structure of the BURFEL output database.

Table 5 Power history of a fuel bundle irradiated in an NRU loop

Irradiation Period		Inner Pin					Outer Pin	
		Segment 1		Segment 2			Segment 3	
Start	End	End Burnup (MWh/kgIHE)	Ave. LP (kW/m)	End Burnup (MWh/kgIHE)	Ave. LP (kW/m)		End Burnup (MWh/kgIHE)	Ave. LP (kW/m)
12/02/1994	18/02/1994	5.0	36.1	4.6	33.2		8.3	41.8
19/02/1994	25/02/1994	11.0	39.7	10.2	36.7		18.4	46.2
26/02/1994	04/03/1994	14.0	38.0	12.9	35.1		23.4	44.2
05/03/1994	11/03/1994	18.7	41.3	17.3	38.2		31.2	47.9
12/03/1994	18/03/1994	23.9	41.9	22.1	38.9		39.8	48.8
Lines removed								
09/02/1995	15/02/1995	147.4	40.2	139.8	40.0		249.0	49.6
16/02/1995	22/02/1995	152.6	39.4	145.0	39.2		258.0	48.2
23/02/1995	01/03/1995	159.1	42.3	151.4	42.1		269.3	51.6
Lines removed								

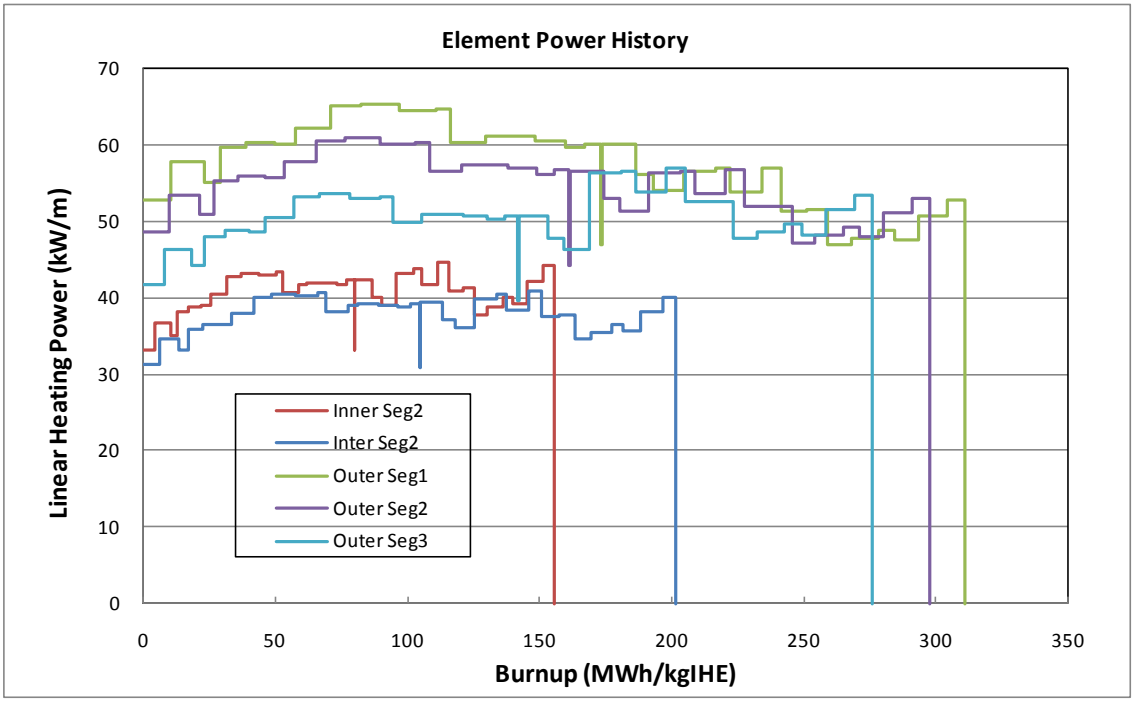

Figure 3 Power versus burnup for selected fuel elements.

The basic theory for the BURFEL code was developed in the 1970's, although the theory and its implementation have evolved to accommodate more complex bundle designs as well as gamma-heating effects, which are important for poisoned fuel and unfuelled burnable neutron poison pins. To obtain the power, burnup, and flux data, the BURFEL code combines the following information:

- The 2D radial power and flux data. These are currently obtained from WIMS-AECL [3].
- The axial cell boundary thermal flux (CBTF) profile along the channel. The flux profile is generally obtained from the TRIAD diffusion code [4] used to model NRU, but it has been obtained from measurements in the past.
- The gamma-heating and heating-power to fission-power ratios. These are currently obtained from 2D neutron-photon calculations using MCNP [5].
- The integrated energy in the end-flux peaks (*i.e.*, EPPR) is estimated based on representative 3D calculations using MCNP. This EPPR allows for a more accurate calculation of the powers in the areas away from the end peak. As will be discussed later, an enhancement to the end-power-peaking calculation could provide the detailed power profile over the end peak.
- The power-to-coolant ratio that the fuel string operates at, as determined from measured calorimetry data (flow, temperature, pressure).

Basically, BURFEL allocates the total string power to the fuel elements in every bundle based on the combined TRIAD (axial) and WIMS (radial) distributions. Optionally, it then derives the coolant temperature and pressure along the channel based on enthalpy and pressure loss evaluations. BURFEL is used only for steady-state calculations.

3. Axial distribution of element powers

BURFEL calculates the linear fission power (*LFP*, kW/m) in a fuel element (*pin*) at a given loop elevation (*z*, cm), as

$$LFP(pin, z) = PGF(pin, bu) \times B \times \varphi(z) \qquad (1)$$

where *PGF*(*pin*, *bu*), kW/m, is the power generation factor (from WIMS) in the *pin* having burnup *bu*; $\varphi(z)$ is the cell boundary thermal flux (CBTF) profile (from TRIAD); and *B* is the normalization factor usually depending on the loop calorimetry power. It is only the TRIAD flux profile that is used to calculate the element power profile in the loop fuel. The element axial power ratio (APR), presented below, may be used to provide more realistic powers in loop bundles. This is particularly true in the case of short regions in BURFEL.

3.1 MCNP model

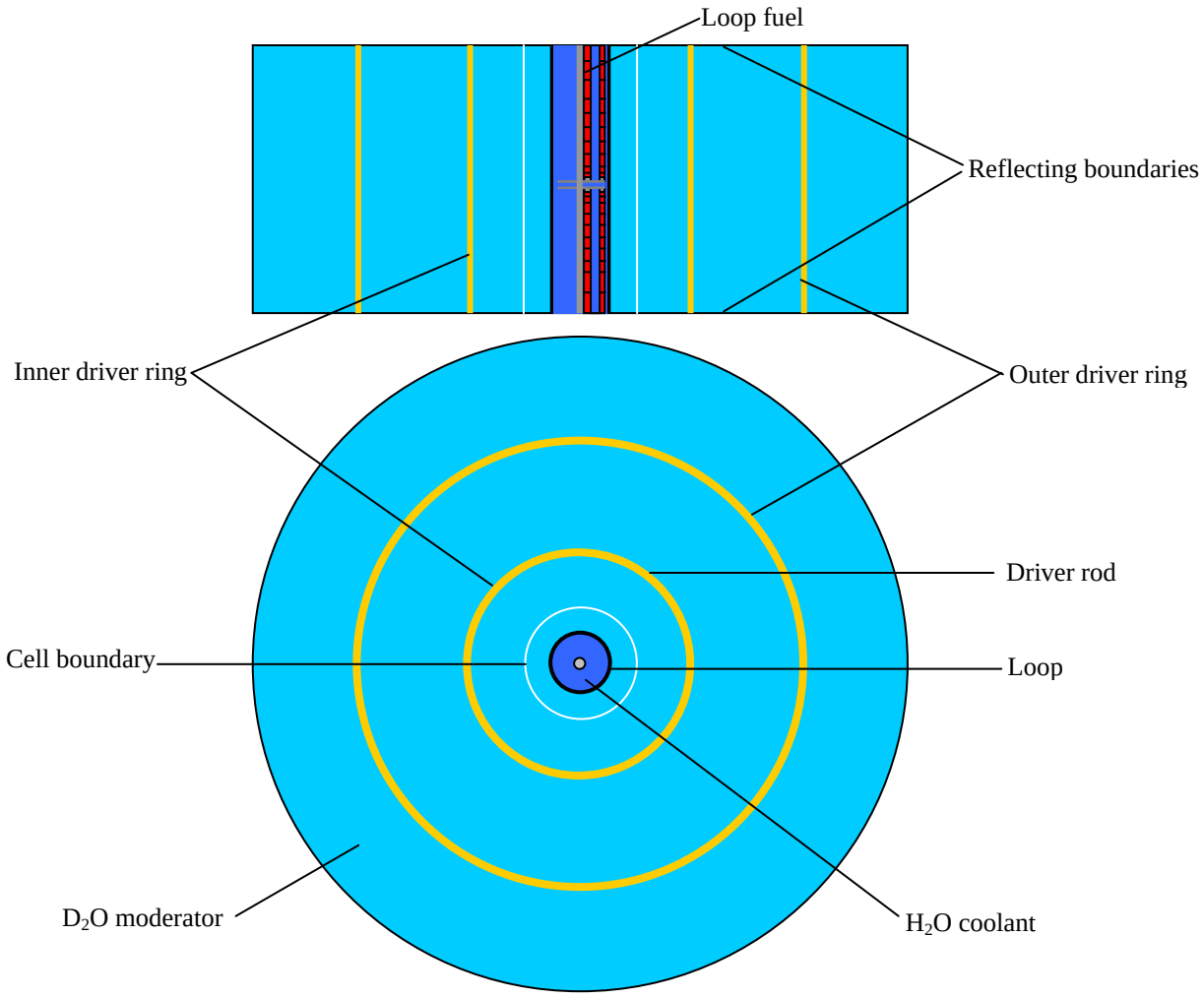

Figure 4 MCNP model for study of power end peaking.

Currently, 3D transport calculations are not used for the entire loop string because of the large computer resources and infrastructure associated with this method. However, an MCNP model of only two adjacent half-bundles loaded in a loop channel (Figure 4), originally used to investigate the power end peaking near the bundle ends, may be used to provide the fission power distribution along each fuel element, from its mid-point to the stack end. All fuel elements are axially sectored to accommodate different materials or compositions (*e.g.*, due to varying fuel burnups). In fact, only the region within the loop cell boundary is modeled accurately with regard to geometries and materials. The outside environment is represented by the D_2O moderator with two driver fuel rings, containing a homogenized mixture (*paste*) of U-235 and B-10 in D_2O, to simulate the two closest surrounding rings of NRU driver fuel rods (as is also used in the WIMS model). The entire model is bounded by two reflecting planes at the upper and lower bundle mid-points, and laterally by a white reflecting cylindrical surface. The U-235/B-10 concentration in the driver fuel paste rings can be adjusted to accurately reflect the NRU environment and maintain the system close to criticality ($k_{eff} \approx 1$). Given a flux at the cell boundary (the cell boundary flux is assumed to be flat over the model length), this MCNP model provides best estimates of the fission powers along the fuel element length, *i.e.*, an axial distribution of the element powers with end-peaking effects (Figure 5). Rigorously, this does not account for an axial variation in the boundary flux, which is expected to be relatively small in practice.

3.2 Axial power ratio

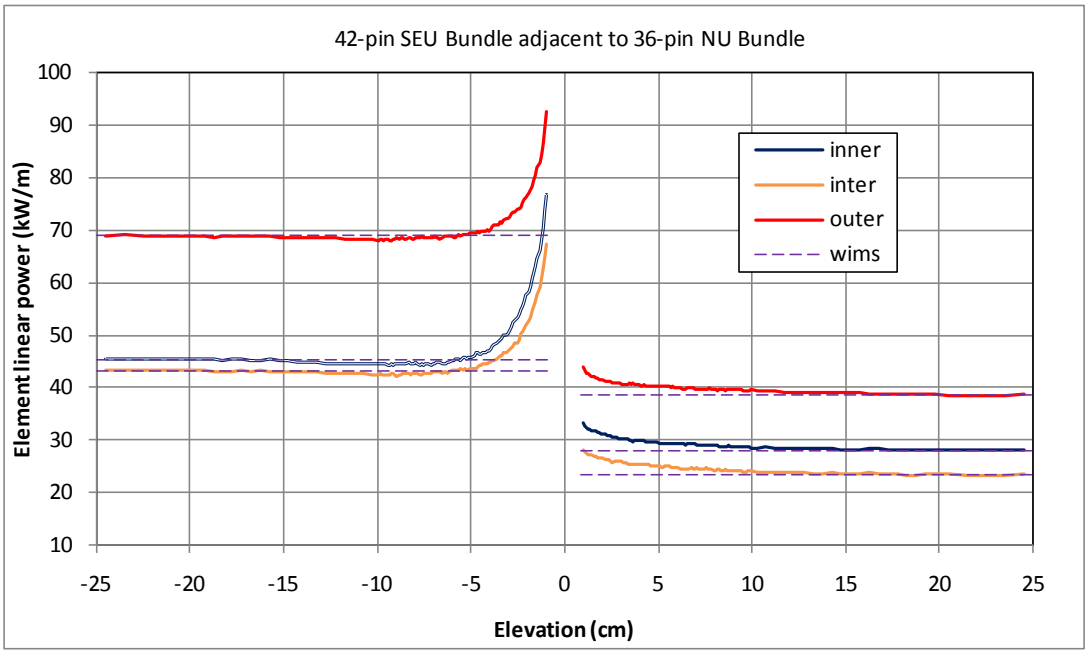

Figure 5 MCNP and WIMS powers.

Under similar flux conditions as for the above MCNP model, the element fission powers from WIMS (*i.e.*, the element PGFs) would be evenly distributed over any uniform element length (Figure 5) as if there were no end-flux peaking effects taking place. Fuel elements are usually long enough such that their central regions are practically out of the influence of the end-peaking

effects. As such, the MCNP fission power (FP) coincides with the WIMS *PGF* at the mid-element. Define the axial power ratio *APR*(*z*) as

$$APR(z) = FP(z) / PGF(z) \times [PGF(mid) / FP(mid)] \quad (2)$$

where the mid-element power ratio, [*PGF*(*mid*) / *FP*(*mid*)], is a scaling factor for the MCNP powers. Figure 6 illustrates such element *APR*(*z*) in a 42-pin bundle containing 2.26%-enriched uranium (SEU) adjacent to a 36-element natural uranium (NU) bundle, with a fuel-to-fuel gap of ~2 cm.

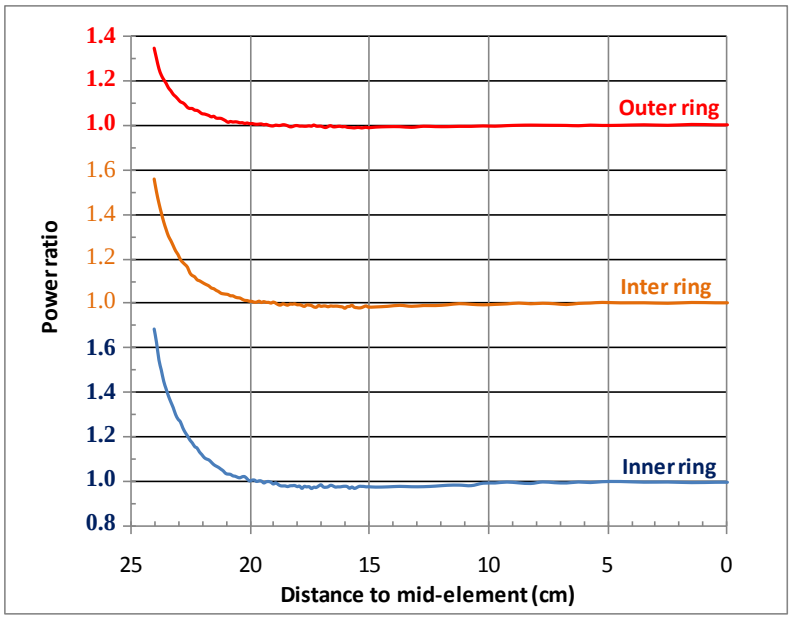

Figure 6 Axial power ratios in 42-element SEU bundle adjacent to NU bundle.

Figure 6 implies that the linear heating powers near the SEU stack ends are significantly greater than the BURFEL predicted values: 70% in the inner ring, 55% in the inter ring, and 35% in the outer ring, or, if averaged over the endmost 1 cm stack length as is customarily done, these increase by a factor of 1.50, 1.39 and 1.22, respectively.

In general, the more accurate element power at any given point can be now calculated as (cf. (1))

$$LFP(pin, z) = PGF(pin, bu) \times B \times \varphi(z) \times APR(z) \quad (3)$$

Figure 7 presents the BURFEL powers and those calculated with end-peaking effects for the string shown in Figure 1. If the maximum BURFEL power in the hottest element is set to meet the string operation value, then the power in its end-pellet is likely to exceed that value. In order to suppress such end-peaking powers, SEU elements may have NU or Dy-doped end-pellets at both stack ends (*e.g.*, in the fifth bundle from the top in Figure 1). The power in such an end-pellet becomes much lower than if the end-pellet was SEU. Note, however, that if an NU end-pellet is used, then a new power peak is created at the SEU stack end. Doping with neutron poisons (*e.g.*, dysprosium) in the end-pellets can effectively eliminate such end-peaking effects.

In Figure 7, the bundles in positions 3 and 5 from the top both contain 2.26% SEU and are adjacent to the same 30-element bundle in position 4, but the position 5 bundle contains NU end-pellets, due to which the average powers over the last 1 cm SEU stack length, as compared to the BURFEL values, have reduced from 1.54, 1.42 and 1.24 in the respective inner, inter and outer rings of bundle 3 to 1.34, 1.26 and 1.15, respectively, in bundle 5.

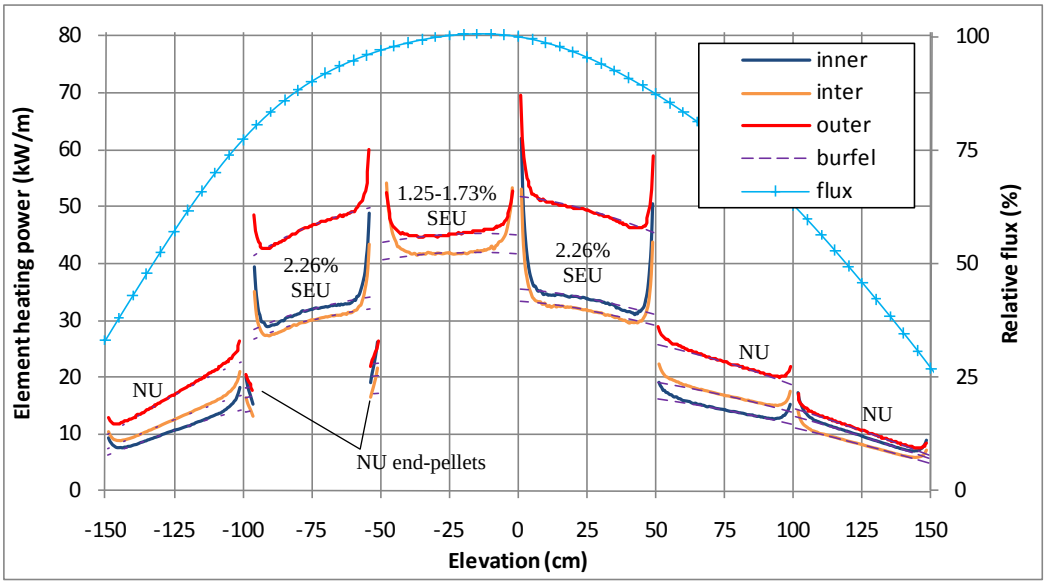

Figure 7 Loop fuel powers.

3.3 Implementation

The current BURFEL can only provide element power distributions exactly following the TRIAD flux shape (Figure 1). If (3) is used instead of (1) in BURFEL, then it can result in more realistic powers in loop fuel elements as shown in Figure 7. For short end regions, the proper burnups could be applied as well.

For the time being, supplementary hand calculations are required to produce the axial power distributions as displayed in Figure 7, with the end-peaking effects accounted for. For that, a more detailed distribution of element powers, *burfel_LHP*(*pin*, *z*), is generated first based on the BURFEL results and CBTF profile. The element linear heating powers (LHP) anywhere in the fuel string that are of interest are then calculated as

$$LHP(pin, z) = burfel\_LHP(pin, z) \times APR(z) \qquad (4)$$

However, burnups in any short regions that are in the end-flux region are not accurately calculated by BURFEL. These can be manually adjusted for input to the next BURFEL cycle. Typically, the element APRs vary slowly and smoothly with irradiation, so it is sufficient to re-calculate these once per irradiation cycle in the NRU.

4. Conclusions

This study gives an insight into axial power distributions in fuel bundles irradiated in the NRU loops. Without the use of end-pellets, power increases near the ends of 2.26% SEU bundles are about 30% higher than the region away from the end-flux peak. The replacement with lower-absorption end-pellets (*e.g.*, NU or depleted uranium) shifts the power peaks deeper into the element and may reduce the size of the peak. The use of Dy-doped end-pellets can remove the end-power-peaking effect.

The axial power ratio, as the 3D MCNP power relative to the 2D WIMS power at a given element location, can be used to obtain more accurate element powers by multiplying with the WIMS-based BURFEL powers.

5. Acknowledgment

This work has been funded by the AECL Nuclear Platform Research and Development Project. The authors would like to thank B. Wilkin and N. Harrison for their contribution.

6. References

[1] W. Shen, "Validation of DRAGON end-flux peaking and analysis of end-power-peaking factors for 37-element, CANFLEX and next-generation CANDU fuels", Proceedings of the 22nd Annual Conference of the Canadian Nuclear Society, Toronto, Ontario, Canada, 2001 June 11-13.

[2] M.D. Atfield, "Calculation of power distribution for experimental bundles in NRU loops", Proceedings of the 22nd Annual Conference of the Canadian Nuclear Society, Toronto, Ontario, Canada, 2001 June 11-13.

[3] J.D. Irish and S.R. Douglas, "Validation of WIMS-IST", Proceedings of the 23nd Annual Conference of the Canadian Nuclear Society, Toronto, Ontario, Canada, 2002 June 3-5.

[4] T.C. Leung and M.D. Atfield, "Validation of TRIAD3 code used for the neutronic simulation of the NRU reactor", Proceedings of the 30nd Annual Conference of the Canadian Nuclear Society, Calgary, Alberta, Canada, 2009 May 31-June 3.

[5] MCNP5 Team, "MCNP – A general Monte Carlo N-particle transport code", Version 5, LANL Report LA-UR-03-1987, 2003.